International Journal of Engineering

Journal Homepage: www.ije.ir

Buckling Behavior of Semi-scale Steel Tank with Carbon Fiber Reinforced Polymer Ring Subjected to Lateral Uniform Pressure Loading

S. Yousefi Khatuni*, H. Showkati

Department of Civil Engineering, Urmia University, Urmia, Iran

P A P E R I N F O	*A B S T R A C T*
	Research on increasing the buckling strength of tanks carrying fluid and also cylindrical shells of thin-walled steel in civil engineering and mechanics is important. This is due to the widespread use of these structures in the industry. Due to the low thickness of the body and also due to the pressure forces entering these tanks, these structures are exposed to lateral buckling. In this research, the use of Carbon Fiber Reinforced Polymer (CFRP) rings to enhance and increase the buckling strength of tanks has been investigated. For this study, a tank with dimensions close to the actual tanks has been built and reinforced by a CFRP ring against the buckling. The results of the experiment indicated that the use of CFRP reinforcing ring considerably enhanced the buckling and post-buckling capacity of the tank. Further, comparing the results obtained from the experimental and numerical analysis and the values extracted from the theoretical relationships suggested that the results are in good agreement.

NOMENCLATURE

D	Bending stiffness of plate	w	Deflection in the z-direction
$E1, E2$ and $E3$	Elasticity modules in the direction of the main axes	Z	Curvature Parameter
$G12, G13$ and $G23$	Shear elastic modules in the direction of the main axes	N_θ	Axial load in the θ-direction
$CFRP$	Carbon fiber reinforced polymer	P_{cr}	Buckling load
L	Height of cylindrical shell	t_f	Thickness of CFRP strips (without resin epoxy)
m	Number of waves in the z-direction	MDF	Medium-density fiberboard
n	Number of waves in the θ-direction	**Greek Symbols**	
N	Number of CFRP layers	σ_{cr}	Critical stress
P_m	Elastic instability pressure for collapse of cylindrical shell	v_{12}, v_{13} and v_{23}	Poisson coefficients in the direction of the main axes
R	Radius of cylindrical shell	ε	Elastic circumferential strain at collapse
t	Thickness of cylindrical shell		

1. INTRODUCTION

Recently, thin-walled structures have found important applications in various branches of engineering [1, 2], which can be attributed to the low thickness of these structures and their high resistance. In thin-walled cylindrical shells, the thickness of the shell thickness is far smaller than its other dimensions. Indeed, in thin-

Corresponding Author Email: s.yousefikhatuni@urmia.ac.ir (S. Yousefi Khatuni)

walled cylindrical shells, the R/t ratio can be considered greater than 500. These structures are used in various industries such as tanks, silos, and chimneys along with cooling towers of power plants. Kalantari and Razzaghi [3] performed a parametric study of the buckling capacity of cylindrical shells with vertical hardening and showed that the buckling capacity of the shells varies exponentially with the adjacent hardening spacing. Louetri et al. [4] have conducted research on cylindrical silos in the hopper section reinforced by fiber reinforced polymeric (FRP) materials. In all cases examined, the use of FRP has been evaluated positively [5].

In order to enhance the buckling strength of shells, engineers recommend the use of longitudinal and circular reinforcement [6]. Lvov et al. [7] investigated the buckling behavior of steel sheathing of a reinforced wall with FRP coating. This research has been done considering the effect of FRP thickness and direction of FRP and buckling axial load loading. Vakili and Showkati [8] conducted a study on the effect of using CFRP reinforcing ring on the elephant foot buckling of cylindrical shells. They reported that the use of CFRP to reinforce the shells has a positive effect. Bhetwal and Yamada [9] studied the use of CFRP to increase the buckling strength of the thin-walled cylindrical shells in which the sides of the shell were reinforced. They observed that the use of CFRP could increase the buckling capacity of the cylindrical shells, which would depend on the thickness and direction of the CFRP. Batikha et al. [10] studied the effect of using FRP on the buckling strength of cylindrical shells with symmetric imperfection. They found that the strength of thin-walled shells with imperfection grew effectively using some FRP materials in the imperfection area. He and Xian [11] conducted experimental studies on the behavior of CFRP rings. The results of the experiments show the failure modes and the required length for the resistance and strain distribution and the load-displacement diagrams and the continuity and slip relations. Showkati and Shahandeh [12] studied on the stiffeners of pipelines under hydrostatic pressure and evaluated the main modes of buckling and extend buckling as well as the subsequent phases of buckling and extension of the yield lines and ultimate failure.

Ghanbari Ghazijahani et al. [13] investigated the partial and full reinforcement effects of the vertical stiffness and the partial thickness of the cylindrical shell subjected to the external pressure. Furthermore, Ghanbari Ghazijahani et al. [14] studied the buckling capacity of cylindrical shells with several transverse waves in different positions of the shell.

Rastgar and Showkati [15] conducted an experimental study to investigate the effect of imperfections on the buckling behavior of cylindrical shells under uniform external pressure on specific specimens.

In this research, in order to enhance the buckling and post-buckling strength of cylindrical shells, a new solution is proposed which resolves most of the abovementioned problems. This solution involves employing rings with CFRP composite materials to increase the buckling and post-buckling strength of steel cylindrical shells against a uniform lateral pressure.

In this paper, using an experimental method and software analysis method plus mathematical approximating relations, use of rings with CFRP composite materials as new materials is recommended to reinforce the steel tank. The aim of this study was experimental and analytical investigation of a semi-scale (Not full scale) steel tank reinforced with CFRP ring. Also, the buckling capacity of the semi-scale tank was evaluated.

2. EXPERIMENTAL PROGRAM

2. 1. Specifications of Experimental Specimen
The test specimen had a diameter of 2000 mm and a height of 1000 mm and the thickness of the tank sheet was 1.5 mm. The number of CFRP layers was 14. The number of CFRP layers was based on the results of nonlinear numerical analysis (ABAQUS) and evaluation of expected performance of the rings. The expected performance of the CFRP rings was the production of sufficient radial stiffness upon radial buckling, and this function was possible by increasing the number of CFRP layers. The position of the CFRP reinforcement ring was in the middle of the tank's height. The width of the CFRP reinforcement ring strip was 50 mm. A two-component epoxy resin was used to attach the CFRP strips to the body of the cylindrical shell. Regarding supporting conditions, the specimen is bounded to the lower part in three directions of tangential, axial and radial but in the upper part, the specimen is bounded radially and tangentially, and the axial displacement is free. Figure 1 represents the tank experimental specimen and 2-component epoxy resin [16] and CFRP strips [17].
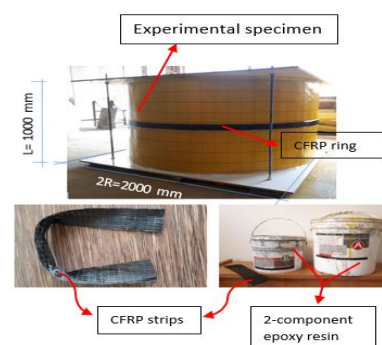

Figure 1. Experimental specimen, and 2-component epoxy resin and CFRP strip

2. 2. Mechanical Properties   Table 1 shows the mechanical properties of the steel plate were obtained by the tensile test of materials (ASTM E8/E8M-15a). Figure 2 represents the tested sample and the utilized device, as well as the stress-strain diagrams. According to the specification provided by the materials manufacturer (QUANTOM®), specifications of CFRP strips [17] and the 2-component epoxy resin [16] to attach the CFRP rings on the cylinders are presented in Tables 2 and 3.

3. TESTING AND EVALUATING THE RESULTS

3. 1. Loading the Experimental Specimen   A vacuum pump was used to investigate the buckling and post-buckling behavior of the experimental tank under the external uniform pressure. This device discharged the air inside the tank with a constant flow rate of 40 m^3/h. Therefore, by discharging the inner air, the atmospheric pressure was uniformly introduced onto the lateral surfaces of the shell. This type of loading occurs in real-condition when the contents of the tank's liquid are drained. Also, since the purpose of this test was investigating the uniform lateral pressure, the loading system was selected in a way that via the retaining bars of the upper and lower sheets of the shell, no vertical

TABLE 2. Mechanical properties of CFRP strips [17]

Product name	QUANTOM®Wrap300
Description	High strength carbon
Thickness	0.167 mm
Tensile strength	4950 MPa
ElastisityModulus	240 GPa
Elangation at breack	1.5%
Areal weight	300 gr/m^2

TABLE 3. The properties of the 2-component epoxy resin [16]

Description	Value
Color	Concrete grey (mixed)
Density	1.5 kg/l (mixed)
Bonding Strength	> 3.5 MPa (Concrete failed)
Compressive Strength	95 MPa (7 days) at 35°C
Tensile & Flexural Strength	> 30 MPa
Service Temperature	-35 to +65°C
Full Cured	After 7 days (at 25°C)
Working Time/Pot Life	60 min. (25°C)

force was introduced to the edges of the shell. Figures 3 and 4 show the steel frame embedded in the bottom and ceiling of the tank to reduce the failure probability of these plates, focus the failure to the tank wall.

TABLE 1. Mechanical properties of steel tensile specimens

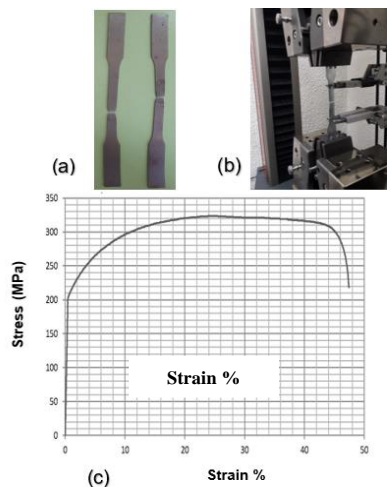| Elastic Modulus	205.9 GPa
Yield Strength	202.5 MPa
Ultimate Strength	327.5 MPa
Rupture Strength	222.5 MPa
Ultimate Strain	48.5%

Figure 3. Steel grid at the bottom of the tank

Figure 2. (a) The two samples, (b) Tensile testing, (c) Stress-strain diagram of material

Figure 4. Steel grid in the roof of the tank

At the installation position of the CFRP ring due to the necessary roughness in the area where the CFRP adhesive is applied, the steel surface of the tank is roughly 15 cm in diameter with a grinding machine. Figure 5 shows the tank after grinding. Figure 6 displays the loading and measurement equipment as well as shows the schematic illustration of the specimen loading and boundary conditions.
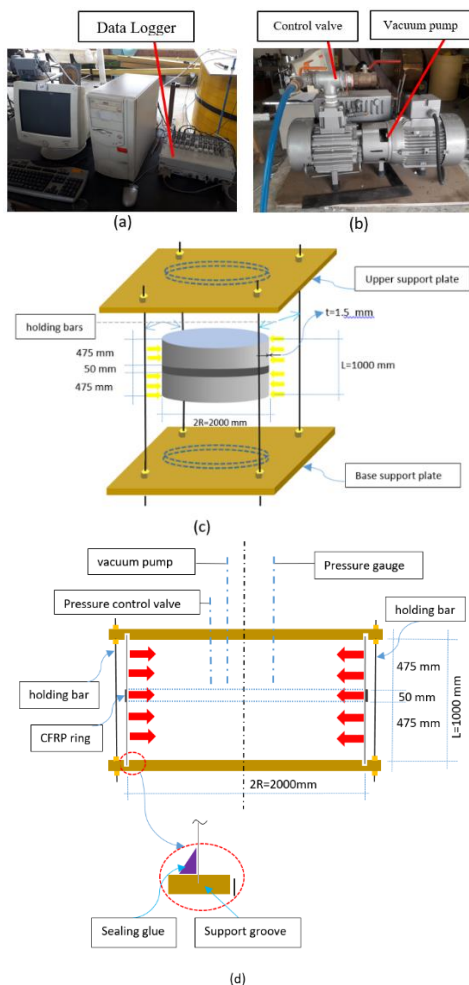

Figure 5. Milling the position of the CFRP ring

Figure 6. (a), (b) A view of the laboratory equipment's, (c), (d) Schematic illustration of the loading and boundary conditions of the experimental specimen

In order to measure the radial displacement as well as the vertical and transverse strain in different parts of the tank, displacement and strain gauges are installed. Further, four LVDTs have been devised to measure the radial displacement of points on the shell. Table 4 reports the specifications of the tested tank. XC and EC represent the symbol of the experimental specimen and the nonlinear numerical analysis specimen, respectively.

3. 2. Test Implementation   After constructing the specimen and implementing the preliminary works and attaching the CFRP reinforcement ring in the middle of the tank, including 14 CFRP layers, the start of the test begins with the tank loading, where the air inside the shell is discharged by the vacuum pump and the uniform external loading is introduced to the shell. Gradually, with continuation of loading, the first buckling waves emerge in the body of the shell, and the buckling phenomenon begins. With further continuation of loading and elevation of the external pressure, ultimately the pressure reaches 24.9 kPa and the number of circumferential waves increases to 12. Finally, due to the fracture of the edge of the MDF (Medium-density fiberboard) plate of upper support, the edge of the shell plate is removed from the upper support groove. As a result, the deboning phenomenon occurs between the CFRP adhesive and the tank body, and the tank undergoes distortion whereby the testing process is terminated. Figure 7 shows buckling and failure of the tank.

TABLE 4. Specifications of the tested specimen

Specimen	XC, EC
R	1000 mm
L	1000 mm
t	1.5 mm
t_f	2.338
Position of CFRP	1/2 L
Number of CFRP Layers (N)	14

Figure 7. failure after ultimate buckling

3. 3. Evaluation of the Experimental Results

Figures 8 and 9 show the horizontal and vertical strain diagrams of the tanks against the applied pressure, respectively. Figures 10a, 10b and 10c demonstrate the location of strain gauges on the tank. As can be observed in Figure 8, the maximum buckling strength of the tank is about 25 kPa. The strain on the CFRP ring indicated a lower value than the other recorded points. Further, the obtained strains are also compressive extending to a pressure of about 21.5 kPa, after which the value of compressive strain decreases which becomes tensional to some extent.

In Figure 11, the diagram of vertical strain gauges of SG1 and SG2 is represented. As observed in Figure 10, the vertical strain values of the SG1 are lower than those of SG2, because the SG1 is located at the bottom of the tank where the extent of displacement is low compared to the upper part of the tank. Therefore, the strain rate is lower than in the upper part. It is observed (see Figure 11) that the radial displacement at the position of LVDT7 has a mild increase at the beginning of loading, and has a minor buckling at the pressure of 12.5 kPa. Then, with the rise in the internal pressure, the displacement is low until the pressure reaches about 15 kPa. After this point, circumferential waves are created mostly in the body of the shell. After this point, a slight fall is observed in the radial displacement, but again with the increase in the internal pressure, the displacement grows, until at the internal pressure of about 25 kPa, the failure of the tank occurs and the test is terminated. The LVDT8 diagram indicates that with initiation of the loading, the displacement of this point is toward the outside of the tank, where this trend continues to a pressure of 18.42 kPa with a displacement of about 0.086 mm. After this point, with continuation of the loading, the displacement decreases while the displacement toward the inside of the tank increases, and this process continues until the failure of the tank. LVDT9 has similar behavior to LVDT7 and LVDT8. With respect to the strain diagrams and the displacements obtained, it is seen that the post-buckling behavior of the tank after the initial buckling was increased and, until the moment of the tank failure, the tank's strength capacity has been rising. (Figures 8, 9 and 11).
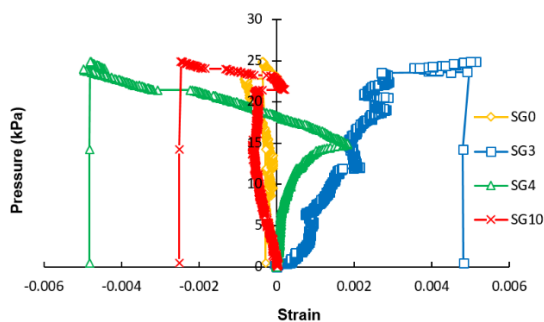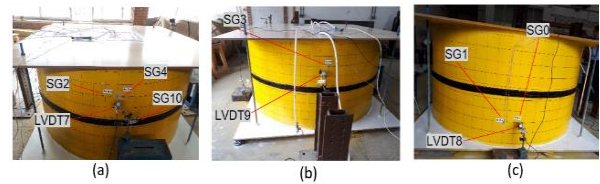

Figure 8. Specimen horizontal strain

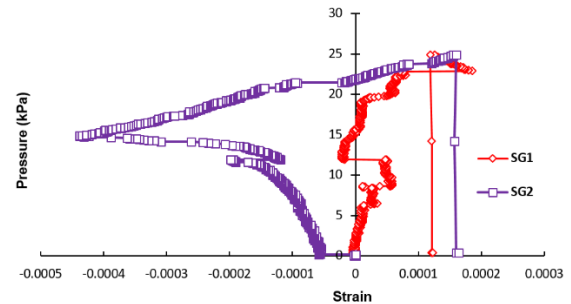**Figure 9.** (a), (b), and (c) Strain gauges and LVDTs positions
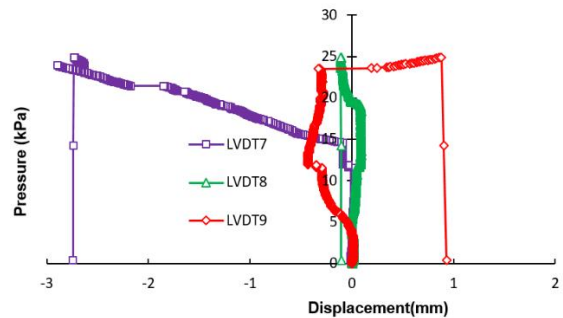

Figure 10. Specimen vertical strain

Figure 11. Radius displacement diagram of the specimen

4. FINITE ELEMENT ANALYSIS

In order to evaluate the buckling behavior of the tank, a numerical analysis is performed on the numerical model of the tank with the same specification of the laboratory specimen using the ABAQUS ver2016 finite element software [18].

The EC abbreviation for nonlinear numerical analysis is used. The geometric and material properties for the EC specimen are modeled as the XC model. The S4R element is used for the modelling of the cylindrical shell. This element is an element of a four-point double-curved shell which can analyze large strains [19]. The behavior of steel materials is modeled bi-linearly in the finite element software. Likewise, the properties of the CFRP material are defined in the software according to Table 2. Hashin's theory is used to model the CFRP material fracture mode.

Boundary conditions are considered at the bottom support and top of the shells a joint. The degree of

freedom is in line with the longitudinal axis of the cylindrical shell. The loading of the specimen is in the form of a uniform external pressure. The type of performed analysis is a nonlinear analysis. Since in the nonlinear buckling analysis consideration of the imperfection is required, so for applying the imperfection, first eigenvalue buckling analysis was conducted. Then, a part of displacements with the first-order mode of the linear buckling was used as imperfection values to perform the nonlinear analysis. Figure 12 represents the finite element model of the modeled tank.

The loading of finite element specimen, like the actual loading of experimental specimen, is a uniform lateral pressure loading. The results obtained from these analyses include the number of circumferential waves observed during the analysis as well as the values of maximum radial displacement and circumferential strain against the pressure.

In Figure 13, the analytical model of the specimen without CFRP reinforcement is represented after loading and buckling. From the nonlinear numerical analysis, the buckling resistance of the tank is obtained to be 18.32 kPa and the number of circumferential waves is 15 Nonlinear analysis model of the specimen reinforced with CFRP is indicated in Figure 14, after loading and buckling. The buckling strength of the tank was obtained 32 kPa from the nonlinear numerical analysis of the tank reinforced with CFRP where the circumferential number of waves was 19.
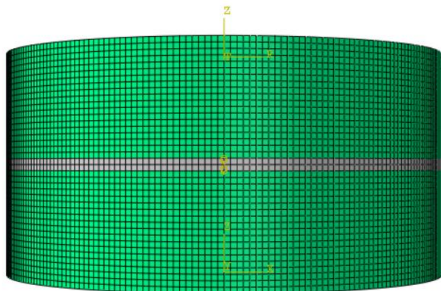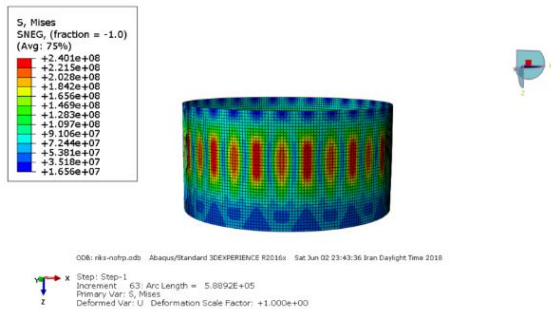
In Figure 15, the radial displacement of a point on the tank against the internal pressure is represented. As observed in Figure 15, the reinforcement of the tank with CFRP rings enhanced the buckling strength of the tank about 75%. This figure indicates that the buckling displacement in the reinforced tank is less than the that of the tank without reinforcement.

5. ANALYTICAL RELATIONS FOR THE BUCKLING OF CYLINDRICAL SHELL

In 1933, Donnell presented an equation to solve the buckling problem of cylindrical shells as follows [20]:

$$D\nabla^8 w + \frac{Et}{R^2}\frac{\partial^4 w}{\partial x^4} + \nabla^4\left(N_x\frac{\partial^2 w}{\partial x^2} + 2N_{xy}\frac{\partial^2 w}{\partial x\,\partial\theta} + N_\theta\frac{\partial^2 w}{\partial \theta^2}\right) = 0 \tag{1}$$

This equation can be used for different conditions of loading. For simple loading of lateral pressure, this equation is presented as follows:
where, $N_x = N_{xy} = 0$ and $N_\theta = pr = \sigma_{cr}t$. Therefore, Equation (1) is written as follows [20]:

$$D\nabla^8 w + \frac{Et}{R^2}\frac{\partial^4 w}{\partial x^4} + \nabla^4\left(N_\theta\frac{\partial^2 w}{\partial \theta^2}\right) = 0 \tag{2}$$

The equation which can be written to indicate the displacement of the cylindrical shell where it can satisfy the simple boundary conditions, is as follows [20]:

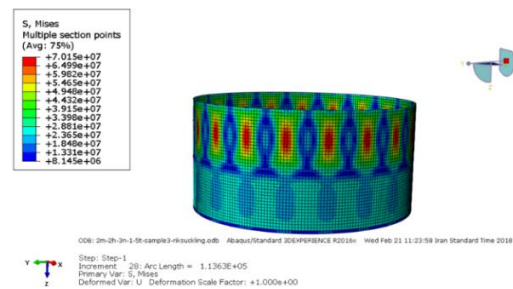$$w = w_{mn}sin\frac{m\pi x}{L}\,sin\frac{n\pi y}{\pi R} \tag{3}$$

Figure 12. Specimen numerical analysis model

Figure 14. Nonlinear numerical analysis model of the reinforced with CFRP specimen after buckling

Figure 13. Numerical analysis model for non-reinforced specimen after buckling
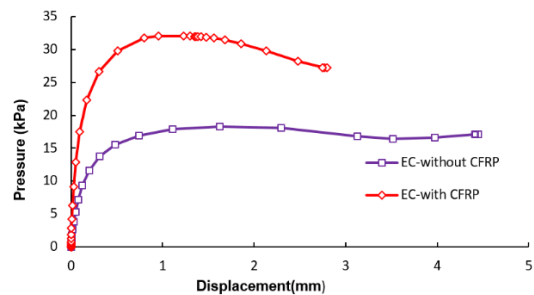

Figure 15. Radius displacement diagrams against internal pressure for reinforced and reinforced specimen

By substituting this relation in Relation (2), we have:

$$\sigma_{cr} = \frac{\pi^2 KE}{12(1-\mu^2)}(t/L)^2 \tag{4}$$

where:

$$K = \frac{(m^2+\beta^2)^2}{\beta^2} + \frac{12Z^2}{\pi^4\beta^2(1+\beta^2/m^2)^2} \tag{5}$$

$$\beta = \frac{nL}{\pi R} \tag{6}$$

$$Z = \frac{L^2}{Rt}\sqrt{(1-\mu^2)} \tag{7}$$

The least value of Equation (5) in obtained by m=1. For short cylinders:

$$K = \frac{(1+\beta^2)^2}{\beta^2} + \frac{12Z^2}{\pi^4\beta^2(1+\beta^2)^2} \tag{8}$$

For short shells, the curvature parameter of Z is zero with Equation (8) obtained as follows:

$$K = (\beta + 1/\beta)^2 \tag{9}$$

If the L/r ratio is increased, then the value of $\beta + 1$ can be approximately substituted with β. So, Equation (8) is written as follows:

$$K = \beta^2 + \frac{12Z^2}{\pi^4\beta^6} \tag{10}$$

Minimizing the above equation toward β gives the following relation:

$$K = 1.038\sqrt{Z} \tag{11}$$

Long cylinders:
For long cylinders, the buckling mode is like circle rings and is in oval shape. Therefore, n=2 and $\beta = \frac{2L}{\pi r}$ as well as Equation (10) decline as follows:

$$K = \beta^2 \tag{12}$$

In Figure 16, the K diagram is represented according to Relations (9), (11), and (12).
Equation (13) is presented by Brush et al. [21] for a cylindrical shell with simple supporting conditions and considering the loading of uniform external lateral pressure.

$$P_{cr} = \frac{1}{R}\left(\frac{(\overline{m}^2+n^2)^2\left(\frac{D}{R^2}\right)}{n^2} + \frac{\overline{m}^4}{n^2(\overline{m}^2+n^2)^2}(1-v^2)C\right) \tag{13}$$

In which:

$$D = \frac{Et^3}{12(1-v^2)} \quad, \quad C = \frac{Et}{(1-v^2)} \quad, \quad \overline{m} = \frac{\pi R}{L}$$

The number of circumferential waveforms obtains from the following equation [21]:

$$n = \sqrt[4]{\frac{6\pi^2\sqrt{1-v^2}}{\left(\frac{L}{R}\right)^2\left(\frac{t}{R}\right)}} \approx 2.74\sqrt{\frac{R}{L}}\sqrt{\frac{R}{t}} \tag{14}$$

According to the experimental relation expanded by the U.S. Navy, the amount of allowable pressure is calculated by the following relation [20]:

$$P_{cr} = \frac{2.42E}{(1-v^2)^{3/4}}\frac{(t/2R)^{2.5}}{[L/2R-0.45(t/2R)^{1/2}]} \tag{15}$$

For structures with a larger ratio of (R/t), Equation (15) is written as follows:

$$P_{cr} = \frac{2.42E}{(1-v^2)^{3/4}}\frac{(t/2R)^{2.5}}{(L/2R)} \tag{16}$$

The British Standard Institute (BSI) [22] has proposed Equation 17 to estimate the P_m (critical load of cylindrical shells), which requires the calculation of the parameter ε. The parameter ε is a function of the values of $2R/t$ and $L/2R$ and is obtained from a design chart that is presented there [22]:

$$P_m = \frac{Et\varepsilon}{R} \tag{17}$$

6. THE EVALUATION OF RESULTS

In Table 5, the summary of the obtained results for the buckling capacity of experimental specimen and numerical analysis as well as the obtained results from the theoretical relations 13, 15 and 17 are represented.
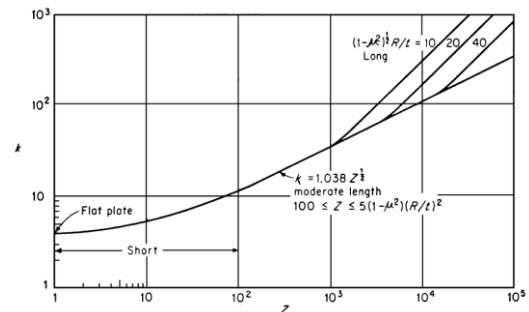

Figure 16. A plot of K [20]

TABLE 5. Comparison of experimental results and theoretical and design code predictions.

Specimen XC	Buckling Strength (kPa)	Difference (%)
Experimental Specimen	25	----
Equation (13) (Without reinforcement)	16.96	47.4
Equation (15) (Without reinforcement)	16.9	47.9
Equation (17) (Without reinforcement)	15.45	61.8
ABAQUS (Without reinforcement)	18.32	36.46

Table 5 shows that the buckling strength of a reinforced experimental specimen is 25kPa.The values obtained from relations 13, 15 and 17, as well as non-linear numerical analysis in Table 5 represent the buckling resistance of the specimen without CFRP reinforcement. The reason for the difference in the ultimate buckling capacity of the tank relates to the termination of the test due to the failure of the upper edge of the support and creation of a de-bonding in the adhesive and the wall of the tank. If the failure at the edge of the top plate of the tank did not occur, it was expected to reach higher buckling strength.

In Figure 17, the experimental results of the semi-tank specimen, theoretical relations, and the numerical analysis are represented for comparison. Figure 17 indicates the experimental results and the results of the theoretical relations along with the results of nonlinear numerical analysis [22]. This figure shows that the experimental specimen has a great post-buckling capacity where the ultimate strength of the experimental specimen is about 25kPa. The overall buckling strength of the experimental specimen shows a 59% increase compared to the theoretical relation. The ultimate strength of the nonlinear numerical analysis specimen is approximately equal to the strength of the experimental specimen.
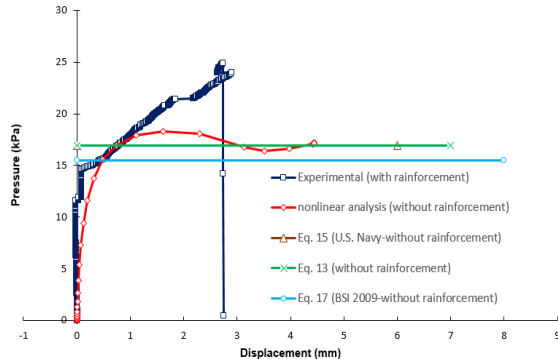

Figure 17. Comparison of the buckling strength of the experimental specimen, numerical analysis, theory relations, and design code

7. CONCLUSION

This paper reports an experimental and numerical study on the structural performance of thin-walled cylindrical shells under uniform external pressure, which intends to investigate the effects of stiffening through CFRP rings in such structures. In this study, use of rings made by CFRP materials was examined to increase the buckling capacity of semi-scale test tanks.

The results obtained from the experimental results, numerical analysis, and approximate theoretical relations confirmed the validity of the conducted work. The

obtained results indicate that the CFRP ring with circumambient function acts properly, which changes the vertical buckling mode of the tank, and thus increases buckling strength.

Ultimately, this research shows that the use of CFRP ring for semi-scale tank with thin wall increases their buckling strength above 36%.

8. ACKNOWLEDGEMENTS

9. REFERENCES

1. Teng, J.G. and Rotter, J.M. eds., Buckling of thin metal shells, CRC Press, 2006.

2. Aghajari, S., Abedi, K. and Showkati, H., "Buckling and post-buckling behavior of thin-walled cylindrical steel shells with varying thickness subjected to uniform external pressure", *Thin-Walled Structures*, Vol. 44, No. 8, (2006), 904–909.

3. Kalantari, Z. and Razzaghi, M. S., "Predicting the buckling capacity of steel cylindrical shells with rectangular stringers under axial loading by using artificial neural networks", *International Journal of Engineering - Transactions B: Applications*, Vol. 28, No. 8, (2015), 1154–1159.

4. Louetri, L., Djeghaba, K. and Gallego Vasquez, E., "Numerical simulation of reinforcement in steel slender silos having concentric hopper with carbon fiber-reinforced polymer composites (study of the silos filling)", *European Journal of Environmental and Civil Engineering*, Vol. 20, No. 7, (2016), 809–830.

5. Ghanbari Ghazijahani, T. and Showkati, H., "An experimental investigation on interactive behavior of thin walled cylindrical shells", *Materialwissenschaft und Werkstofftechnik*, Vol. 44, No. 5, (2013), 386–394.

6. Foryś, P., "Optimization of cylindrical shells stiffened by rings under external pressure including their post-buckling behaviour", *Thin-Walled Structures*, Vol. 95, (2015), 231–243.

7. Lvov, G., Pupazescu, A., Beschetnikov, D. and Zaharia, M., "Buckling Analysis of a Thin-walled Cylindrical Shell Strengthened by Fiber-reinforced Polymers", *Materiale Plastice*, Vol. 52, No. 1, (2015), 28–31.

8. Vakili, M. and Showkati, H., "Experimental and numerical investigation of elephant foot buckling and retrofitting of cylindrical shells by FRP", *Journal of Composites for Construction*, Vol. 20, No. 4, (2015), 04015087(1–9).

9. Bhetwal, K.K. and Yamada, S., "Effects of CFRP reinforcements on the buckling behavior of thin-walled steel cylinders under compression", *International Journal of Structural Stability and Dynamics*, Vol. 12, No. 1, (2012), 131–151.

10. Batikha, M., Chen, J.F. and Rotter, J. M., "Elastic buckling of FRP-strengthened cylinders with axisymmetric imperfections", In Proceedings of Asia-Pacific Conference on FRP in Structures, APFIS2007, (2007), 12–14.

11. He, J. and Xian, G., "Debonding of CFRP-to-steel joints with CFRP delamination", *Composite Structures*, Vol. 153, (2016), 12–20.

12. Showkati, H. and Shahandeh, R., "Experiments on the buckling

behavior of ring-stiffened pipelines under hydrostatic pressure", *Journal of Engineering Mechanics*, Vol. 136, No. 4, (2009), 464–471.

13. Ghanbari Ghazijahani, T., Jiao, H. and Holloway, D., "An experimental study on externally pressurized stiffened and thickened cylindrical shells", *Thin-Walled Structures*, Vol. 85, (2014), 359–366.

14. Ghanbari Ghazijahani, T., Dizaji, H.S., Nozohor, J. and Zirakian, T., "Experiments on corrugated thin cylindrical shells under uniform external pressure", *Ocean Engineering*, Vol. 106, (2015), 68–76.

15. Rastgar, M. and Showkati, H., "Field Study and Evaluation of Buckling Behavior of Cylindrical Steel Tanks with Geometric Imperfections under Uniform External Pressure", *International Journal of Engineering - Transactions C: Aspects*, Vol. 30, No. 9, (2017), 1309–1318.

16. QUANTOM® EPR 3301, Version 2017, http://quantom.co.uk/wp-content/uploads/2019/03/EPR-3301.pdf.

17. QUANTOM® Wrap 300C, Version 2017, http://quantom.co.uk/wp-content/uploads/2018/10/online-catalouge-for-WRAP-300C-v2.02.pdf.

18. ABAQUS/Standard User's Manual, Version 6.16, Dassault Systèmes Simulia Corp., Providence, RI., 2016.

19. Showkati, H. and Ansourian, P., "Influence of primary boundary conditions on the buckling of shallow cylindrical shells", *Journal of Constructional Steel Research*, Vol. 36, No. 1, (1996), 53–75.

20. Jawad, M., Theory and design of plate and shell structures, Springer Science & Business Media, 2012.

21. Brush, D.O., Almroth, B.O. and Hutchinson, J.W., Buckling of bars, plates, and shells, Mc Grow Hill, New York, 1975.

22. BSI, Specification for Unfired Fusion-Welded Pressure Vessels, British Standard Institution, United Kingdom, 2009.

Buckling Behavior of Semi-scale Steel Tank with Carbon Fiber Reinforced Polymer Ring Subjected to Lateral Uniform Pressure Loading

S. Yousefi Khatuni, H. Showkati

Department of Civil Engineering, Urmia University, Urmia, Iran

چکیده

تحقیقات در رابطه با افزایش مقاومت کمانشی مخازن حامل مایعات و همچنین پوسته‌های استوانه‌ای جدار نازک فولادی در مهندسی عمران و مکانیک حائز اهمیت است. این موضوع به علت استفاده گسترده از این مخازن در صنعت می‌باشد. به علت ضخامت کم و همچنین به علت میدان فشاری وارد بر مخازن این سازه‌ها در معرض کمانش جانبی می‌باشند. در این تحقیق استفاده از حلقه‌های CFRP جهت افزایش مقاومت کمانشی مخازن مورد مطالعه قرار گرفته است. برای این تحقیق یک مخزن با ابعاد مشابه مخازن واقعی ساخته شده و توسط یک حلقه CFRP در وسط ارتفاع مخزن در مقابل کمانش جانبی مقاوم سازی شده است. نتایج بدست آمده نشان می دهد که استفاده از حلقه CFRP بصورت موثری مقاومت کمانشی و پس کمانشی مخزن را افزایش می‌دهد. بعلاوه مقایسه نتایج بدست آمده از آزمایش با نتایج تحلیل عددی غیرخطی و روابط تئوری و نیز روابط آئین‌نامه‌ای مطابقت خوبی را نشان می‌دهند.

doi: *10.5829/ije.2019.32.10a.10*